Selected Paper

Photoisomerization and Fluorescence Properties of Hemiindigo Compounds Having Intramolecular Hydrogen Bonding

Masashi Ikegami and Tatsuo Arai*

Department of Chemistry, University of Tsukuba, Tsukuba, Ibaraki 305-8571

Received February 24, 2003; E-mail: arai@chem.tsukuba.ac.jp

Intramolecularly hydrogen bonded hemiindigo compounds **2**–**4** were prepared and their photochemical behavior was investigated. *Z*-**2** did not undergo isomerization, while **3** underwent isomerization mutually between the *Z*-isomer and *E*-isomer in solution to exhibit a color change between greenish yellow and reddish orange in benzene. Introduction of a formyl group at the 2-position of the pyrrole ring of **3** brought about the increase in the fluorescence quantum yield and fluorescence lifetime by a factor of 10, and the decrease of the quantum yield of isomerization of **4** in benzene. In addition, introduction of the formyl group affects the thermal stability. The intramolecular hydrogen bonding can be used to construct a novel photochromic molecule.

Photochromic compounds have received considerable attention as basic materials for photochromic memory or switching devices in recent years.[1–6] Most of the photochromic behavior is based on electrocyclizations. For example, Irie et al. reported photochromic properties of diarylethenes with heterocyclic aryl groups based on a photochemical cyclization reaction.[3,4]

The photoisomerization of the C=C double bond is a basic photochemical reaction that shows the change in the absorption spectrum by *Z*–*E* isomerization.[7,8] The control of the isomerization mode and the absorption maximum of the olefins are important in developing photochromic materials based on the isomerization around the C=C double bond.

It has been reported that the mode of photoisomerization that results in the one-way *cis*-to-*trans* isomerization of aromatic olefins depends on the subsitituent on the C=C double bond, as observed in 2-styrylanthracene.[9] The one-way *cis*-to-*trans* isomerization took place in the triplet excited state, and the mode of the isomerization was controlled by the triplet energies of the aromatic ring substituted on the ethylenic carbon.[9]

Intramolecular hydrogen bonding can be used to control the isomerization mode and for changing the absorption maximum between the *E*-isomer and *Z*-isomer.[10–18] For example, an olefin with a pyrrole ring and a pyridine ring (**1**) exhibited one-way $E \rightarrow Z$ isomerization due to the presence of intramolecular hydrogen bonding in the *Z*-isomer.[13] *Z*-**1** exhibited an absorption maximum at a longer wavelength ($\lambda_{max} = 372$ nm) than that of the *E*-isomer ($\lambda_{max} = 347$ nm) in benzene.[13] However, the difference in absorption maxima between the *Z*- and *E*-isomer was too small to exhibit the practical color change in the visible region.

Hemiindigo derivatives **2** and **3** with an absorption maximum in the visible region have already been prepared,[19] but their absorption spectra, as well as their photochemical properties, have not been reported. We have reported the assignment and some photochemical properties of **2** and **3** in the preliminary paper.[16,17]

Indigo is one of the most important dyes, exhibiting a deep blue color with excellent stability. The stability of indigo is related to the presence of two intramolecular hydrogen bonds in the molecule. Therefore, *N*-alkyl substituted indigo derivatives or thioindigo derivatives, which did not have intramolecular hydrogen bonding, underwent isomerization mutually between the *Z*-isomer and *E*-isomer.[20–24]

Since indigo could not undergo isomerization on photoirradiation, the study of the photochemical reaction of related compounds is important to construct photochromic molecules having absorption spectra at longer wavelengths as well as to explore the role of intramolecular hydrogen bonding in the photochemical behavior of the indigo derivatives. Intramolecularly hydrogen bonded aromatic compounds can undergo intramolecular hydrogen atom transfer in the excited state to give a tautomer.[25–29] Therefore, the photostability of indigo should be the consequence of the ultra-fast deactivation in the intramolecular hydrogen bonding from the excited state.

We wish to report here the full account of photochemical and photophysical behavior of **2** and **3**, in addition to that of **4**, where **3** and **4** underwent mutual photoisomerization between the *Z*-isomer and *E*-isomer and exhibited a color change between greenish yellow and reddish orange (Scheme 1). Thus, the absorption spectra of the hemiindigo derivatives appeared in the visible region, and the isomerization around the C=C double bond resulted in a color change. Furthermore, we have found that the substitution of a formyl group controls the photochemical behavior, as observed for **4**.

Experimental

Materials and Solvents. The hemiindigo derivatives **2**, **3**, and **4** were synthesized by aldol condensation from 3-indolyl acetate and an appropriate aromatic aldehyde to yield only *Z*-isomers.[19] Pyrrole-2,5-dicarboxaldehyde was prepared by a Vilsmeier reaction from pyrrole.[30] *E*-**3** was obtained by irradiation of a benzene solution of *Z*-**3** at 366 nm to give a photostationary mixture with a high ratio of *E*-isomer. The obtained hemiindigo was purified by

Published on the web September 15, 2003; DOI 10.1246/bcsj.76.1783

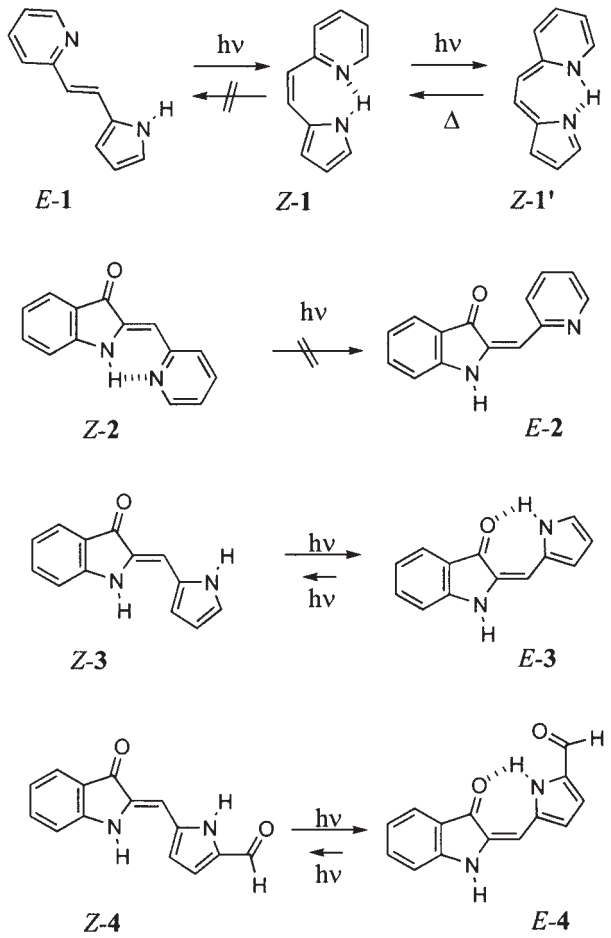

Scheme 1.

column chromatography and recrystalized from ethanol.

(*Z*)-2-(2-Pyridylmethylidene)indolin-3-one (*Z*-**2**): ^{1}H NMR (DMSO-d_6, 200 MHz) δ 6.58 (1H, s), 6.87 (1H, t, $J = 8.0$ Hz), 7.25 (2H, m), 7.70 (4H, m), 8.70 (1H, m), 10.3 (1H, br). mp 153–154 °C.

(*Z*)-2-(2-Pyrrolylmethylidene)indolin-3-one (*Z*-**3**): ^{1}H NMR (DMSO-d_6, 200 MHz) δ 6.31 (1H, m), 6.71 (1H, s), 6.87 (2H, m), 7.07 (1H, m), 7.13 (1H, d, $J = 8.2$ Hz), 7.50 (2H, m), 9.30 (1H, s), 11.40 (1H, s). mp 200–202 °C. *E*-**3**: δ 6.34 (1H, m; pyrrole-H), 6.71 (1H, m), 6.81 (1H, s), 6.87 (1H, m), 7.06 (1H, d, $J =$ 8.4 Hz), 7.25 (1H, m), 7.47 (1H, m), 7.63 (1H, d, $J = 8.4$ Hz), 9.78 (1H, br), 13.35 (1H, br). mp 191–193 °C.

(*Z*)-2-[(2-Formyl-5-pyrrolyl)methylidene]indolin-3-one (*Z*-**4**): ^{1}H NMR (DMSO-d_6, 200 MHz) δ 6.63 (s, 1H), 6.91 (1H, t, $J = 7.4$ Hz), 7.02 (1H, m) 7.15 (2H, m), 7.53 (2H, m), 9.50 (s, 1H), 9.70 (br, 1H), 12.4 (br, 1H). mp 224–226 °C. ESI-MS Calcd for $C_{14}H_{11}N_2O_2$ $[M + H]^+ = 239.0821$. Found: 239.0812.

In spectroscopy, Dotite Spectrosol or Luminasol were used as solvents without further purification.

Measurement. Absorption and fluorescence spectra were measured on a JASCO Ubest-55 and on a Hitachi F-4000 fluorescence spectrometer, respectively.

Laser flash photolyses were performed by using an excimer laser (Lambda Physik LPX-100, 308 nm, 20 ns fwhm) or excimer laser pumped dye laser (Lambda Physik LEXtra-100, 308 nm, 20 ns fwhm and Lambda Physik Scanmate, stilbene 3, 425 nm, or QUI, 390 nm, 10 ns fwhm) as excitation light sources and a pulsed xenon arc (Ushio UXL-159) was used as a monitoring light source. A photomultiplier (Hamamatsu R-928) and a storage oscilloscope (Iwatsu TS-8123) were used for the detection.

Fluorescence lifetimes were determined with a picosecond laser system consisting of a titanium sapphire laser (Spectra Physics 3900 "Tsunami") operated with a CW Ar^+ laser (Spectra Physics 2060), a frequency doubler (SP-390), a pulse selector (SP-3980; ≈2 ps fwhm), and a streak scope (Hamamatsu C4334).

An Oxford Cryostat model DN-1704 and temperature controller ITC-4 were used for the low temperature experiment.

DSC measurement was performed with a Seiko DSC-220 and data module SSC-5500H.

A JASCO Ubsest 55 equipped with a HAAKE K was used for the determination of the rate constant of thermal isomerization.

NMR and ESI-MS spectra were measured on a Varian Gemini 2000 and Applied Biosystems QStar/Pulsar *i*, respectively.

Quantum yield of fluorescence was determined by using anthracene ($\Phi_f = 0.27$)[31] as a fluorescence standard.

Quantum yield of isomerization was determined with 366-nm light from a 400 W high-pressure mercury lamp through UV-35 and U-360 filters. The sample solution was deaerated by bubbling argon and irradiated for 5–15 min to keep the conversion within 10%. Light intensity was determined by tris(oxalato)ferrate(Ⅲ) actinometory.[32] The concentration of each isomer was determined by high-performance liquid chromatography through a column (TOSO ODS-80TS) eluting with acetonitrile/water = 4/1.

Results

Absorption Spectra. Absorption spectra of **2**, **3**, and **4** are shown in Fig. 1. The absorption maximum of *Z*-**2** appeared at 477, 477, and 482 nm in benzene, acetonitrile, and methanol, respectively. The absorption maximum of *Z*-**2** was slightly shifted to longer wavelengths in methanol compared to that in benzene.

The absorption spectrum of *E*-**3** was slightly depended on the solvent. The maximum appeared at 524, 523, and 531 nm in benzene, acetonitrile, and methanol, respectively, giving a reddish orange color in these solvents. On the other hand, *Z*-**3** exhibited a greenish yellow color in benzene. The absorption maximum of *Z*-**3** appeared at 495 nm in methanol and 470 nm in benzene, indicating that the intermolecular hydrogen bonding between *Z*-**3** and methanol decreases the excitation energy.

Compound **4**, having a formyl group at the 2-position of the pyrrole ring of compound **3**, exhibited similar absorption spectra to **3** for both the *E*- and *Z*-isomer, as shown in Fig. 1.

The absorption spectrum of *E*-**3** appeared at longer wavelengths than that of *Z*-**3**, probably due to the presence of intramolecular hydrogen bonding. Intramolecular hydrogen bonding plays an important role in lowering the excitation energy in intramolecularly hydrogen bonded isomers.[10–18] The difference in absorption maximum between the *E*-form and *Z*-form of **3** and **4** seemed to be larger than that of typical aromatic ethenes. Usually, the absorption maximum of the *Z*-isomer appears at shorter wavelengths than that of the *E*-isomer, because of the steric hindrance in the *Z*-isomer.[7] For example, the absorption maximum of stilbene appeared at 282 nm and 298 nm for the *Z*-isomer and *E*-isomer, respectively, in benzene.

Photoisomerization. The *Z*-isomer of **2** did not undergo

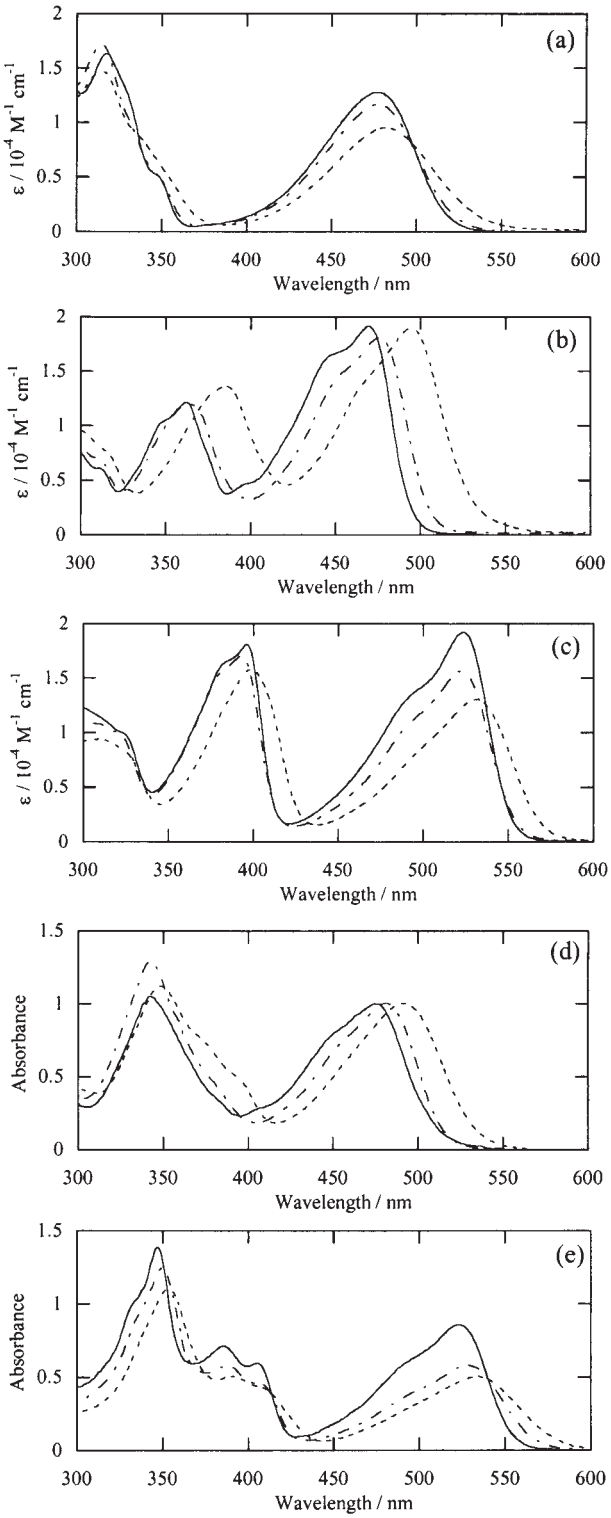

Fig. 1. Absorption spectra of *Z*-**2** (a), *Z*-**3** (b), *E*-**3** (c), *Z*-**4** (d) and *E*-**4** (e) in benzene (solid line), acetonitrile (dashed line) and methanol (dotted line).

isomerization to give an *E*-isomer in methanol or in benzene after irradiation at any wavelength. The fluorescence spectrum was not detected for *Z*-**2** at room temperature. On direct irradiation in benzene, **3** underwent mutual isomerization between the *Z*-isomer and *E*-isomer. Compound **4** also underwent mutual isomerization between the *Z*-isomer and *E*-isomer. The photostationary isomer ratio $([E]/[Z])_{PSS}$ and the quantum yields of isomerization after irradiation at 366 nm are summarized in Table 1.

After 366-nm light irradiation, the absorption band of *Z*-**3** appeared at 470 nm, decreased with a concomitant increase of *E*-**3**, appearing at 524 nm, to give a photostationary isomer mixture with a very high composition of *E*-isomer, $([E]/[Z])_{PSS} = 99/1$, in benzene, as shown in Fig. 2a. On the other hand, *E*-**3** underwent isomerization to give the *Z*-isomer with the *Z*-isomer composition as high as 85% after irradiation at 546 nm, as shown in Fig. 2b. The isosbestic points appeared at 366, 408, and 483 nm in benzene. The $([E]/[Z])_{PSS}$ value after irradiation at 366 nm decreased in polar and protic solvents and is 99/1, 95/5, and 89/11 in benzene, acetonitrile, and methanol, respectively.

Compound **3** exhibited almost one-way *Z*-to-*E* isomerization after irradiation with 366 nm light, where both the *Z*-isomer and *E*-isomer have similar absorption coefficients. The considerably large difference between $\Phi_{Z\rightarrow E}$ and $\Phi_{E\rightarrow Z}$ is the reason for the almost one-way isomerization. However, a very high ratio of *Z* isomer at the photostationary state ($([E]/[Z])_{PSS} = 15/85$) was observed after irradiation at 546 nm, where *E*-**3** has a much higher absorption coefficient than *Z*-**3**. Therefore, the irradiation wavelength affected the photostationary state isomer composition to give ~99% of the *E*-isomer and ~85% of the *Z*-isomer with irradiation at 366 nm and 546 nm, respectively. The repetition characteristics of an absorption spectrum by alternate irradiation between 366 nm and 546 nm are shown in Fig. 3. The ratio of *Z* isomer depended on the irradiation time and excitation wavelength. In this experimental condition, it took 5 min and 60 min to reach a photostationary state on irradiation at 366 nm and 546 nm, respectively.

The quantum yields of *Z*-to-*E* isomerization of **3** were 0.3 in all the solvents examined, whereas those of *E*-to-*Z* isomerization were ~0.003, 0.02, and 0.05 in benzene, acetonitrile, and methanol, respectively. With irradiation at 366-nm light, **4** underwent mutual isomerization to give the photostationary state (Fig. 4 and Table 1). The irradiation time dependence of the absorbance at the maximum wavelength of 475 nm, 482 nm, and 492 nm in benzene, acetonitirile, and methanol, respectively, were observed against irradiation time. The time dependence of the *Z*-isomer composition was obtained from these results and was plotted in Fig. 5. In benzene, the initial slope of the absorbance change of *Z*-**4** was similar to that of *Z*-**3** in benzene. The quantum yields of *Z*-to-*E* isomerization of **4** were estimated to be 0.17, 0.05, and 0.009 in benzene, acetonitrile, and methanol, respectively by comparing the initial slope of the time development of isomerization. The quantum yield of isomerization of **4** was strongly dependent on the solvent and decreased in acetonitrile and methanol.

Ground State Properties. In order to investigate the energetic profile in the ground state, the DSC experiments were performed at different rising temperature rates (2.5–7 °C min^{-1}). Thus, the energy difference between *Z*-**3** and *E*-**3** in the ground state was determined to be 7 kcal mol^{-1}. In addition, the activation energy for *Z*-to-*E* isomerization was calculated to be 16 kcal mol^{-1} by a similar method reported by

Table 1. Quantum Yields of Isomerization and Isomer Ratio at Photostationary State on Irradiation for **3** and **4**

	Compound **3**				Compound **4**		
	$\Phi_{Z\to E}$	$\Phi_{E\to Z}$	$([E]/[Z])_{PSS}$ ($\lambda_{ex} = 366$ nm)	$([E]/[Z])_{PSS}$ ($\lambda_{ex} = 546$ nm)	$\Phi_{Z\to E}$	$\Phi_{E\to Z}$	$([E]/[Z])_{PSS}$ ($\lambda_{ex} = 366$ nm)
Benzene	0.31	0.003	99/1	15/85	0.17	0.002	96/4
Acetonitrile	0.32	0.02	95/5		0.05	0.004	93/7
Methanol	0.33	0.05	89/11		0.009	0.001	90/10

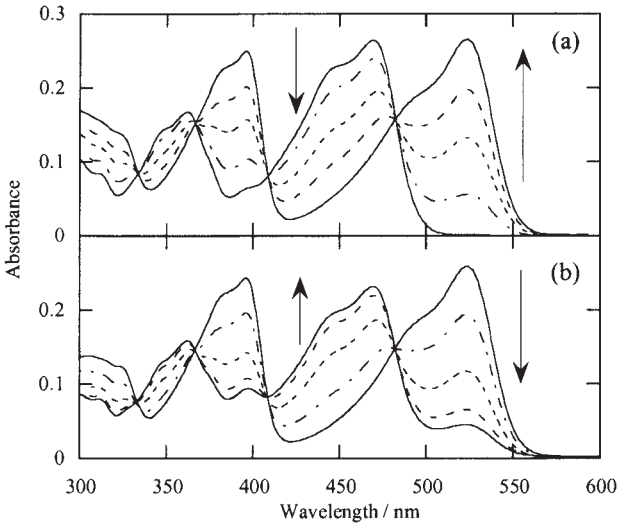

Fig. 2. Change of absorption spectrum of *Z*-**3** (a) and *E*-**3** (b) on irradiation at 366 nm and 546 nm, respectively in benzene under argon.

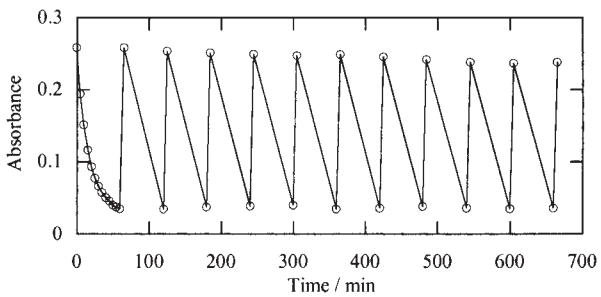

Fig. 3. Repetition characteristics of **3** by alternate irradiation at 366 nm and 546 nm of high pressure mercury lamp in benzene under argon monitored at 524 nm.

Kissinger.[33]

Compound **3** isomerized thermally between the *Z*-isomer and *E*-isomer at room temperature in methanol, 2-propanol, and acetonitrile, while **3** was thermally stable in benzene. The rate constant of isomerization was determined from the change in the absorption spectrum at constant temperature. The time development of the absorption maximum of the *E*-isomer was traced, and the rate constant for thermal *Z*-to-*E* isomerization was calculated by the first order rate law.

In addition, the equilibrium constant between the *E*-isomer and *Z*-isomer was estimated by the relationship of $K = k_{Z\to E}/k_{E\to Z}$. Furthermore, the enthalpy (ΔH) and the entropy differences (ΔS) between the *Z*- and *E*-isomer were calculated by the van't Hoff equation (1). The results are summarized in Table 2.

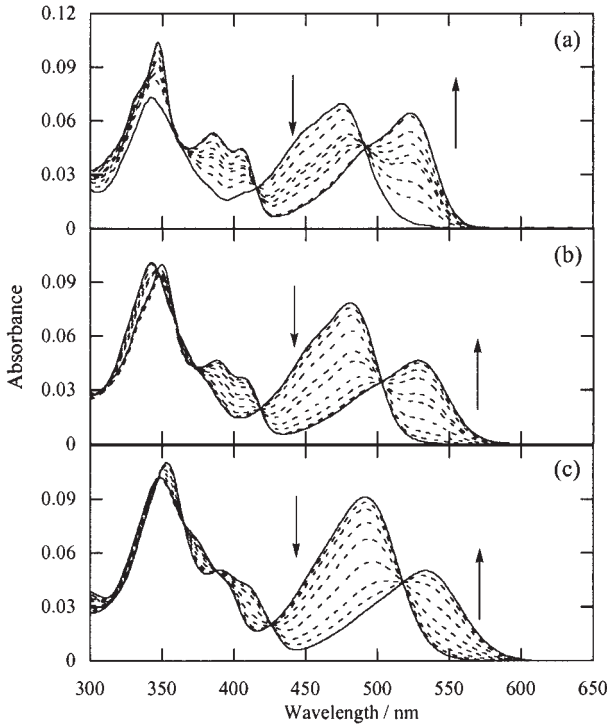

Fig. 4. Change of absorption spectrum of *Z*-**4** in benzene (a), acetonitrile (b) and methanol (c) on irradiation at 366 nm.

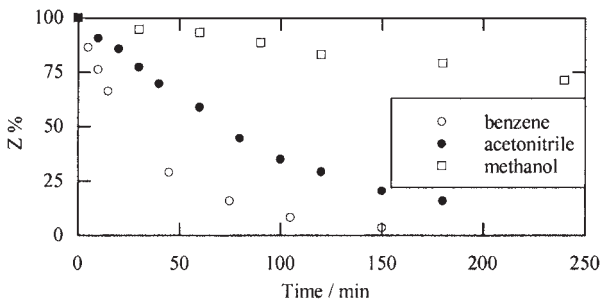

Fig. 5. Time development for *Z*-to-*E* isomerization of *Z*-**4** on irradiation at 350 nm in benzene, acetonitrile and methanol.

$$\ln K = -\frac{\Delta H}{RT} + \text{const.} \quad (1)$$

Triplet State Behavior. Upon laser photolysis, a transient absorption spectrum was not observed in compounds **2**–**4**, indicating that compounds **2**–**4** did not undergo intersystem crossing upon direct irradiation. Thus, laser flash photolysis

Table 2. Rate Constants of Isomerization and Thermodynamic Parameters for *Z*-to-*E* Isomerization of **3**

		A[a]	E_a[b]	ΔH[b]	ΔS[c]	[E]/[Z][d]
Methanol	$Z \rightarrow E$	4.4×10^{11}	23.4	0.85	1.4	27/73
	$E \rightarrow Z$	2.2×10^{11}	22.5			
2-Propanol	$Z \rightarrow E$	1.2×10^{12}	24.9	0.4	1.3	50/50
	$E \rightarrow Z$	6.4×10^{11}	24.5			
Acetonitrile	$Z \rightarrow E$	9.4×10^{6}	17.6	−1.4	−3.4	65/35
	$E \rightarrow Z$	5.3×10^{7}	19.0			
Solid (DSC)	$Z \rightarrow E$		16	−7		

a) In s^{-1}. b) In kcal mol^{-1}. c) In cal mol^{-1} K^{-1}. d) At 298 K.

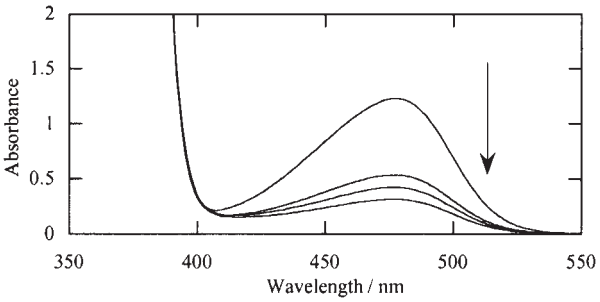

Fig. 6. Absorption spectrum change of *Z*-**2** on Michler's ketone sensitization with 390 nm light.

was performed in the presence of a triplet sensitizer in benzene.

Figure 6 shows the change in the absorption spectra of *Z*-**2** (1.0×10^{-4} M) on Michler's ketone (0.06 M) sensitization with a 390-nm laser pulse in benzene. The intense absorption band observed below 400 nm and the absorption band at 480 nm were assigned to the absorption spectra of Michler's ketone and *Z*-**2**, respectively. During the laser photolysis experiments with a 390-nm laser pulse, the absorption band at 480 nm decreased, and the solution color changed from orange to pale yellow. This means that *Z*-**2** decomposed in the triplet excited state, probably by hydrogen abstraction to give a radical species.

Triplet sensitization experiments on *Z*-**3** and *E*-**3** were also performed in benzene. The transient absorption spectra of *Z*-**3** (6×10^{-5} M) on Michler's ketone (1×10^{-4} M) sensitization with a 308-nm laser pulse are shown in Fig. 7. Immediately after laser excitation, a decrease in absorption of *Z*-**3** was observed at 470 nm and the absorbance at 530 nm corresponding to the absorption of *E*-**3** gradually increased. The change in the transient absorption spectrum indicates that the *Z*-to-*E* isomerization occurred in the triplet excited state. Actually, the *E*-isomer was detected by HPLC experiments after laser excitation of *Z*-**3** in the presence of Michler's ketone.

On the other hand, *E*-**3** (5×10^{-4} M) gave a transient absorption spectra with the maximum wavelength at 600 and 680 nm on biacetyl (0.14 M) sensitization (Fig. 8) using a 425-nm laser pulse in benzene. The oxygen quenched the transient species appeared at 600 nm, which was assigned to the triplet excited state. The other transient species can be assigned to the radical, which was produced by the hydrogen abstraction reaction of the carbonyl group of the triplet state **3**. The absorption spectrum of *E*-**3** decreased after the irradiation

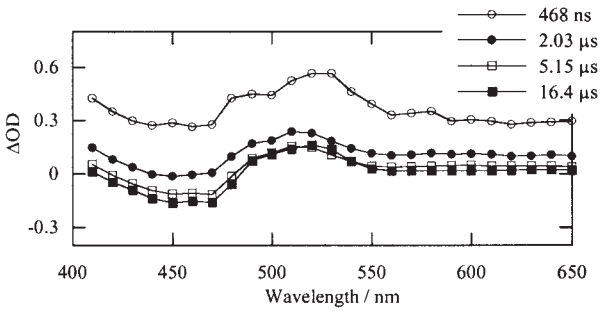

Fig. 7. Transient absorption spectra of *Z*-**3** on Michler's ketone sensitization in benzene.

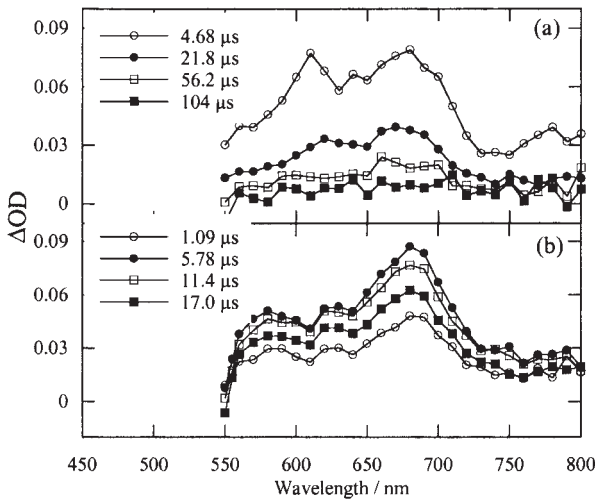

Fig. 8. Transient absorption spectra of *E*-**3** on biacetyl sensitization under argon (a) and under air (b) in benzene.

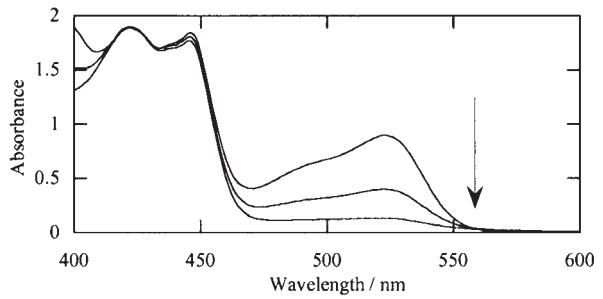

Fig. 9. Absorption spectrum change of *E*-**3** on biacetyl sensitization with 425-nm light.

with the triplet sensitizer as shown in Fig. 9, similar to the case of *Z*-**2** (Fig. 6). The energy diagram of **3** in the triplet excited state is shown in Fig. 10.

The rate constant of triplet quenching from benzil ($E_T = 53$ kcal mol^{-1}) to *E*-**3** in benzene was determined to be 7.4×10^9 M^{-1} s^{-1}. Therefore, the triplet energy transfer from benzil to *E*-**3** occurred by a diffusion controlled process.[26–29] Thus, the triplet energies of **2** and **3** could be estimated to be lower than that of benzil ($E_T = 53$ kcal mol^{-1}). Both **2** and **3** did not exhibit a phosphorescence spectrum at 77 K.

Fluorescence Properties. Fluorescence and fluorescence excitation spectra of **3** and **4** in toluene are shown in Figs. 11

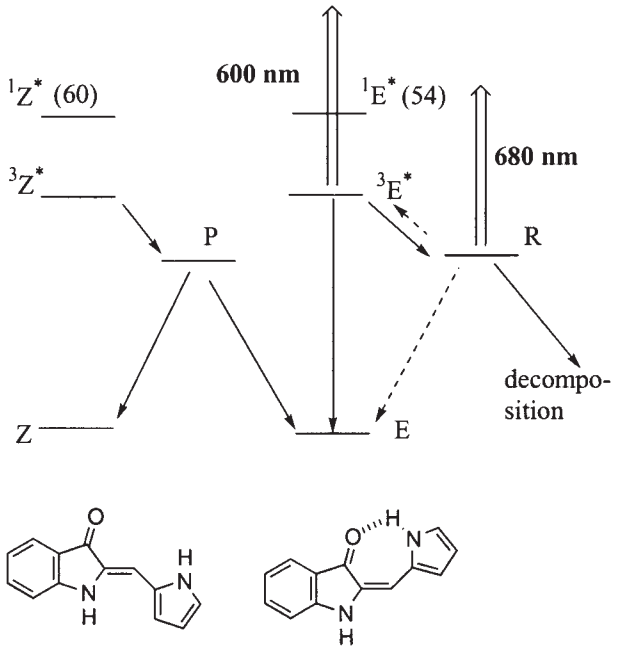

Fig. 10. Energy diagram of **3** in the triplet excited state.

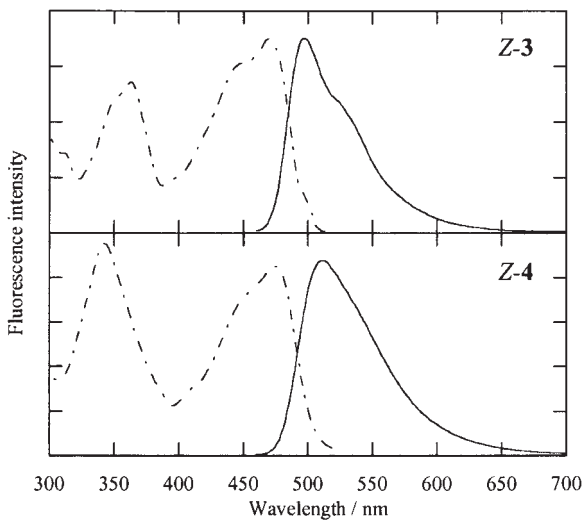

Fig. 11. Fluorescence and fluorescence excitation spectra of *Z*-**3** and *Z*-**4** in toluene at 295 K.

and 12. The singlet energies are almost the same for **3** and **4**, and the fluorescence excitation spectra are similar to the absorption spectra.

The quantum yield of fluorescence and the fluorescence lifetime of compounds **3** and **4** were measured and the results are summarized in Table 3. Fluorescence emission was not observed for **2** at room temperature.

The fluorescence lifetime of **4** was ca. 10 times longer than that of **3**, and the quantum yield of fluorescence of **4** was 10 times larger than that of **3** in toluene. These results indicate that the rate constant of the non-radiative deactivation pathway decreased as a result of the introduction of the formyl substituent to the pyrrole ring. The rate constant of fluorescence emission was calculated by Eq. 2. In this equation, k_f, τ_f, and Φ_f stand for the rate constant of natural fluorescence decay, lifetime of the singlet excited state, and quantum yield of fluorescence, respectively.

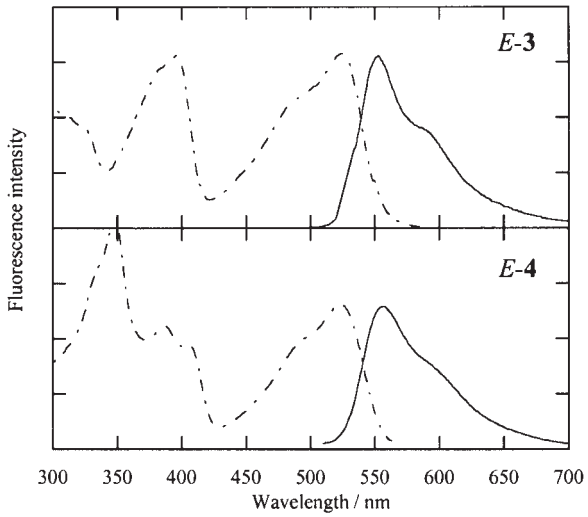

Fig. 12. Fluorescence and fluorescence excitation spectra of *E*-**3** and *E*-**4** in toluene at 295 K.

$$k_f = \Phi_f/\tau_f \quad (2)$$

Thus, k_f was estimated to be 2.5×10^7 s^{-1} and 7.1×10^7 s^{-1}, respectively, for *E*-**3** and *Z*-**3**, and to be 1.9×10^7 s^{-1} and 5.9×10^7 s^{-1}, respectively, for *E*-**4** and *Z*-**4** in toluene. The value of k_f was nearly the same for **3** and **4**.

The temperature dependence of the fluorescence lifetime in toluene was observed from 298 K to 185 K and the results are summarized in Table 4. The fluorescence lifetime of *E*-**3** increased from 210 ps to 2.9 ns while decreasing the temperature from 295 K to 185 K. The fluorescence lifetime of *E*-**4** also increased from 4.6 ns to 8.1 ns while decreasing the temperature from 295 K to 185 K.

Discussion

Energetic Profile in the Ground State. The difference in enthalpy (ΔH) between *Z*-**3** and *E*-**3** was estimated to be 7 kcal mol^{-1} from the results of the DSC experiment. On the other hand, *Z*-**3** was more stable than *E*-**3** by 0.85 kcal mol^{-1} in methanol, as determined from the equilibrium constant in solution (Table 2). These results indicate that the intermolecular hydrogen bonding between *Z*-**3** and methanol stabilizes the ground state of *Z*-**3**. The positive value of the entropy difference (ΔS) observed for the *Z*-to-*E* isomerization in methanol, 1.4 cal mol^{-1} K^{-1}, could be explained by the existence of intermolecular hydrogen bonding between *Z*-**3** and methanol. In 2-propanol, the enthalpy difference (ΔH) between *Z*-**3** and *E*-**3** is smaller than that in methanol probably because the bulkier alkyl group of 2-propanol prevents the formation of intermolecular hydrogen bonding.

The activation energy (E_a) for the *Z*-to-*E* isomerization in the ground state in methanol, 2-propanol, and acetonitrile was calculated by the Arrhenius equation. The E_a and the frequency factor (A) for the *Z*-to-*E* isomerization were calculated to be 23.4 kcal mol^{-1} and 4.4×10^{11} s^{-1}, respectively, in methanol and 24.9 kcal mol^{-1} and 1.2×10^{12} s^{-1}, respectively, in 2-propanol. In acetonitrile, E_a and A for the *Z*-to-*E* iso-

Table 3. Spectroscopic Parameters of **3** and **4** at 295 K

			λ_{max}/nm									
			Abs.	Fluo.	E_s[a]	Φ_f	Φ_{iso}	Φ_{nr}[b]	τ_f/ns	k_f[c,d]	k_{iso}[c,d]	k_{nr}[c,d]
	Benzene	*Z*	470	500	59.0	0.023	0.31	0.36	0.35	6.6	180	100
		E	524	554	53.1	5.9×10^{-3}	0.003	0.99	0.21	2.8	1.4	470
	Toluene	*Z*	470	498	58.8	0.025	0.31	0.36	0.35	7.1	180	100
		E	525	553	53.1	5.2×10^{-3}	0.003	0.99	0.21	2.5	1.4	470
3	Acetonitrile	*Z*	477	514	57.6	2.6×10^{-3}	0.32	0.36				
		E	523	560	52.6	2.1×10^{-3}	0.02	0.96				
	Methanol	*Z*	495	533	55.9	5.9×10^{-4}	0.33	0.34				
		E	531	574	51.6	6.4×10^{-4}	0.05	0.90				
	Chloroform	*Z*	476	514	57.6	2.0×10^{-3}						
		E	524	560	52.6	1.8×10^{-3}						
	Toluene	*Z*	475	511	58.1	0.29	0.17	0.37	4.9	5.9	6.9	7.6
		E	524	556	52.8	0.086	0.002[e]	0.91	4.6	1.9	0.09	20
4	Acetonitrile	*Z*	482	543	56.4	0.04	0.05	0.86				
		E	528	590	51.7	4×10^{-3}	0.004[e]	0.99				
	Methanol	*Z*	491	585	54.5	8×10^{-4}	0.009	0.98				
		E	534	630	50.7	3×10^{-5}	0.001[e]	0.99				

a) In kcal mol^{-1}. b) $\Phi_{nr} = 1 - (2\Phi_{iso} + \Phi_f)$. c) In 10^7 s^{-1}. d) $k_f = \Phi_f/\tau_f$, $k_{iso} = 2\Phi_{iso}/\tau_f$, $k_{nr} = \Phi_{nr}/\tau_f$. e) $\Phi_{E\to Z} = \Phi_{Z\to E}(\varepsilon_Z/\varepsilon_E)([Z]/[E])_{PSS}$. Φ_f: Quantum yield of fluorescence, Φ_{iso}: Quantum yield of isomerization, Φ_{nr}: Quantum yield of non-radiative deactivation (internal conversion).

Table 4. Temperature Dependence of Fluorescence Lifetime of *E*-**3** and *E*-**4** in Toluene

E-**3**		*E*-**4**	
Temp./K	τ_f/ns	Temp./K	τ_f/ns
295	0.21	295	4.6
276	0.27	288	4.8
267	0.31	280	5.2
258	0.36	270	5.6
251	0.44	260	6.1
241	0.54	250	6.8
233	0.73	210	7.9
220	0.96	200	8.0
211	1.2	185	8.1
200	1.8		
190	2.4		
185	2.9		

merization were calculated to be 17.6 kcal mol^{-1} and 9.4×10^6 s^{-1}, respectively.

Compound **3** underwent mutual isomerization between the *E*-isomer and *Z*-isomer at room temperature in methanol. However, introduction of the formyl group increases the thermal stability in a protic solvent, and therefore, compound **4** was stable even in methanol.

Effects of Formyl Group on the Fluorescence Emission and Isomerization. Introduction of the formyl group to compound **3** may increase the efficiency of intersystem crossing. However, compound **4** did not exhibit a transient absorption spectrum in the laser flash photolysis experiment at room temperature. In addition, compound **4** underwent mutual isomerization between the *Z*-isomer and *E*-isomer without decomposition. As mentioned above, *E*-**3**, having intramolecular hydrogen bonding, underwent decomposition upon triplet sensitization. Therefore, the efficiency of intersystem crossing of compound **4** is estimated to be almost negligible.

Both *Z*-**3** and *E*-**3** exhibited fluorescence emission with a quantum yield of 0.025 and 5.2×10^{-3}, respectively, in toluene. The introduction of the formyl group at the 2-position of the pyrrole ring of **3** increased the fluorescence quantum yield and fluorescence lifetime by a factor of 10. It was reported that the quantum yield of fluorescence of **1** increased by a factor of 100 as a result of the introduction of a formyl group at the 2-position of pyrrole ring.[14]

The increase in the quantum yield of fluorescence by the introduction of a formyl group is attributed to the decrease of the non-radiative decay rate constant (k_{nr}), as shown in Table 3.

Hydrogen bonding should accelerate the rate constants of non-radiative deactivation due to the high frequency of vibrational motion. Inoue et al. reported that the fluorescence quantum yield of aminoanthraquinone or aminofluorenone derivatives decreased in alcoholic solvents by intermolecular hydrogen bonding interaction.[34,35]

The proximity effect can also explain the acceleration of non-radiative deactivation.[36,37] When the energy difference between the excited $n\pi^*$ state and $\pi\pi^*$ state is small, non-radiative decactivation can be accelerated by proximity. For example, the observation that the quantum yield of fluorescence of *trans*-2-styrylpyridine and *trans*-4-styrylpyridine is smaller than that of *trans*-stilbene is explained by the perturbation of the $\pi\pi^*$ state with a nearly isoenergetic $n\pi^*$ state, resulting in greatly enhanced non-radiative decay.[38]

In the hemiindigo compounds, the rate constant of non-radiative deactivation decreased with the introduction of a formyl group in both the *E* and *Z* isomers. The explanation of the above mechanisms need further investigation.

The introduction of the formyl group affects the fluorescence as well as the isomerization behavior. In acetonitrile

and methanol, the fluorescence emission was strongly quenched. As mentioned above, quantum yields of the *Z*-to-*E* isomerization of **3** were 0.3 in all the solvents examined. However, the quantum yield of the *Z*-to-*E* isomerization of **4** was strongly dependent on the solvent, and was estimated to be 0.17, 0.05, and 0.009 in benzene, acetonitrile, and methanol, respectively. It was believed that intermolecular hydrogen bonding between methanol and **4** would accelerate the non-radiative deactivation. Our results show both the fluorescence and isomerization efficiencies were lowered.

Temperature Effect on the Non-Radiative Deactivation Processes. Intramolecular hydrogen bonding accelerates the deactivation pathway from the excited state, and, therefore, the quantum yield of fluorescence emission of a hydrogen bonded isomer is sometimes smaller than the compound without hydrogen bonding, as previously reported.[10–18]

The fluorescence lifetime of *E*-**3** ($\tau_s = 210$ ps) is shorter than that of *Z*-**3** ($\tau_s = 350$ ps) in benzene, indicating some role of the intramolecular hydrogen bonding in the deactivation from the excited singlet state of *E*-**3**. Fluorescence emission of *Z*-**2** was not observed at room temperature. In addition, *Z*-to-*E* isomerization did not occur in *Z*-**2** with photoirradiation, indicating that *Z*-**2** underwent ultra fast deactivation from the excited singlet state through intramolecular hydrogen bonding. However, at 77 K in ethanol glass, *Z*-**2** exhibited a fluorescence emission with a maximum at 520 nm and a lifetime of ca. 8 ns, indicating that deactivation through intramolecular hydrogen bonding was suppressed with decreasing temperature.

These results indicate that intramolecular hydrogen bonding plays an important role in the deactivation from the singlet excited state in *Z*-**2** and *E*-**3**.

As described in the results, quantum yields of the *E*-to-*Z* isomerization of *E*-**3** and *E*-**4** were estimated to be less than 0.01 in toluene. In addition, the intersystem crossing process was negligible. Therefore, we can postulate that the singlet lifetime (τ_f) of the *E*-form is explained by Eq. 3, while k_{nr} is the rate constant of non-radiative deactivation through intramolecular hydrogen boning and is dependent on temperature.

$$\tau_f = 1/(k_f + k_{nr}) \quad (3)$$

The fluorescence lifetime of *E*-**3** increased from 210 ps to 2.9 ns with decreasing temperature from 295 K to 185 K in toluene. The fluorescence lifetime of *E*-**4** increased from 4.6 ns to 8.1 ns with decreasing temperature from 295 K to 185 K in toluene. The Arrhenius plot of $\ln(k_{nr})$ vs T^{-1} gave a straight line, as shown in Fig. 13. The activation energy and frequency factor for k_{nr} were calculated to be 2.7 kcal mol^{-1} and 5.2×10^{11} s^{-1}, respectively, for *E*-**3**, and 1.4 kcal mol^{-1} and 2.2×10^{9} s^{-1}, respectively, for *E*-**4** from Eq. 4.

$$\ln(k_{nr}) = \ln(1/\tau_f - k_f) = \ln A - E_a/RT \quad (4)$$

The fluorescence lifetime of *E*-**4** becomes constant at 8.0 ns under 140 K. As a result, the values from 295 K to 250 K were used for the calculation of the activation parameter.

The frequency factor of non-radiative deactivation for *E*-**4** was smaller than that of *E*-**3** by a factor of 100 in toluene. This result indicates that the frequency of the vibrational mode attributed to non-radiative deactivation was lowered by the introduction of the formyl group, probably due to the inductive effect of the formyl group or hydrogen bonding interaction between the formyl group and the NH group in the pyrrole ring.

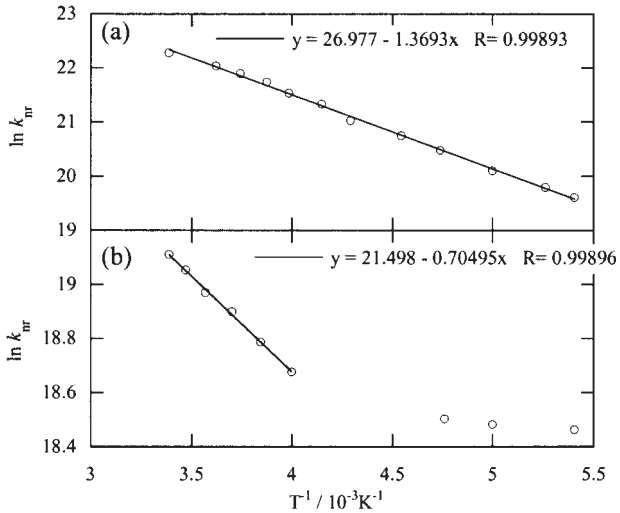

Fig. 13. Arrhenius plot for non-radiative deactivation from the singlet excited state of *E*-**3** (a) and *E*-**4** (b) in toluene.

Potential Energy Surface of *E–Z* Isomerization. In non-polar solvents, such as benzene and toluene, the stabilization energy of *E*-**3** was estimated to be 7 kcal mol^{-1} due to the presence of intramolecular hydrogen bonding from the DSC experiment. On the other hand, *Z*-**3** was stabilized at 0.85 kcal mol^{-1} in methanol due to the presence of intermolecular hydrogen bonding. Potential energy surfaces of the *E–Z* isomerization based on the singlet excitation energy estimated from fluorescence and fluorescence excitation spectra are shown in Fig. 14.

Quantum yields of *Z*-to-*E* isomerization of **3** were 0.31 and 0.33 in benzene and methanol, respectively, while those of **4** were 0.17 and 0.009 in benzene and methanol, respectively. Since the rate constants of fluorescence (k_f) of **3** and **4** in toluene were almost the same, the rate constants of non-radiative deactivation and isomerization in the singlet excited state were strongly dependent on solvent polarity and hydrogen bonding. As summarized in Table 3, introduction of the formyl group brings about a decrease of the rate constant of non-radiative deactivation as well as the rate constant of isomerization in the singlet excited state. On the basis of the results of the solvent dependence of isomerization of **4**, the rate constant of non-radiative deactivation was accelerated in a polar protic solvent such as methanol, probably due to the intermolecular hydrogen bonding interaction.

Conclusion

Compound **3** exhibited almost one-way *Z*-to-*E* isomerization upon irradiation with 366-nm light, although *Z*-**3** and *E*-**3** have similar absorption coefficients at 366 nm, due to the considerably large difference between $\Phi_{Z\rightarrow E}$ and $\Phi_{E\rightarrow Z}$. However, **3** gives a photostationary mixture with a very high ratio of *Z*-isomer to *E*-isomer, 85:15, upon irradiation at 546 nm, where *E*-**3** has a much higher absorption coefficient than *Z*-**3**.

Introduction of the formyl group to the pyrrole ring of **3** improves the thermal stability in solution. The quantum yield of

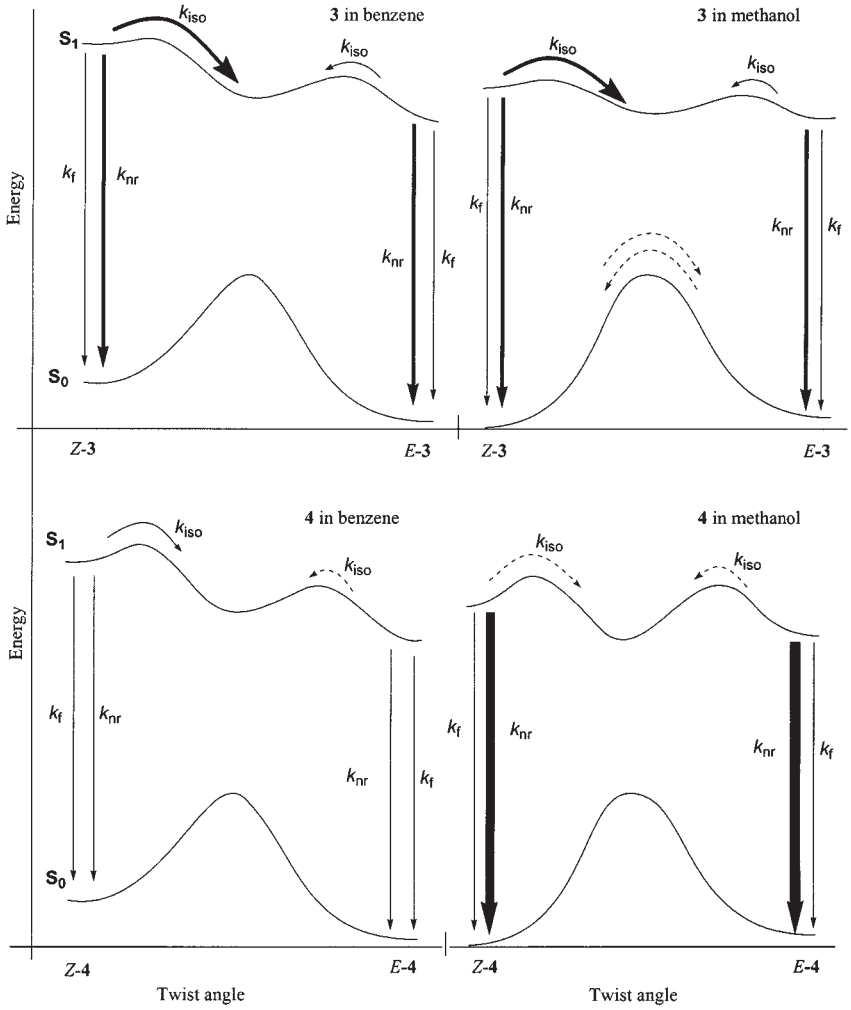

Fig. 14. Potential energy surface of *E–Z* isomerization of **3** and **4** in benzene and in methanol.

isomerizaiton of **4** in methanol was lowered by a factor of 100 compared to that in benzene, while the quantum yield of isomerization of **3** was almost the same in methanol and benzene. Introduction of the formyl group resulted in an increase in the quantum yield of fluorescence and fluorescence lifetime.

On the basis of the these findings, it was found that the intramolecular hydrogen bonding plays an important role in constructing photochromic compounds having an absorption band in the visible region, and the substituents and solvents affect their photochromic properties.

This work was supported by a Grant-in-Aid for Scientific Research on Priority Areas (No. 417) from the Ministry of Education, Culture, Sports, Science and Technology (MEXT), by Research Foundation for Opto-Science and Technology and by the Asahi Glass Foundation.

References

1 J. C. Crano and R. Guglielmetti, "Organic Photochromic and Thermochromic Compounds Vol. 1, 2," Kluwer Academic/Plenum Press, New York (1999).

2 H. Dürr and H. Bouas-Laurent, "Photochromism: Molecules and Systems," Elsevier, Amsterdam (1990).

3 M. Irie, *Chem. Rev.*, **100**, 1685 (2000).

4 M. Irie and K. Uchida, *Bull. Chem. Soc. Jpn.*, **71**, 985 (1998).

5 Y. Yokoyama, *Chem. Rev.*, **100**, 1717 (2000).

6 A. Mishra, R. K. Behera, P. K. Behera, B. K. Mishra, and G. B. Behera, *Chem. Rev.*, **100**, 1973 (2000).

7 J. Saltiel, A. S. Waller, and D. F. Sears, Jr., *Photochem. Photobiol. A: Chem.*, **65**, 29 (1992).

8 D. H. Waldeck, *Chem. Rev.*, **91**, 415 (1991).

9 T. Arai and K. Tokumaru, *Chem. Rev.*, **93**, 23 (1993).

10 F. D. Lewis, B. A. Yoon, T. Arai, T. Iwasaki, and K. Tokumaru, *J. Am. Chem. Soc.*, **117**, 3029 (1995).

11 T. Arai, M. Obi, T. Iwasaki, K. Tokumaru, and F. D. Lewis, *J. Photochem. Photobiol. A: Chem.*, **96**, 65 (1996).

12 T. Arai, M. Moriyama, and K. Tokumaru, *J. Am. Chem. Soc.*, **116**, 3171 (1994).

13 M. Obi, H. Sakuragi, and T. Arai, *Chem. Lett.*, **1998**, 169.

14 T. Arai and Y. Hozumi, *Chem. Lett.*, **1998**, 1153.

15 Y. Yang and T. Arai, *Tetrahedron Lett.*, **39**, 2617 (1998).

16 T. Arai and M. Ikegami, *Chem. Lett.*, **1999**, 965.

17 M. Ikegami, T. Suzuki, Y. Kaneko, and T. Arai, *Mol. Cryst. Liq. Cryst.*, **345**, 437 (2000).

18 M. Ikegami and T. Arai, *J. Chem. Soc., Perkin Trans. 2*, **2002**, 342.

19 A. R. Katrinzky, Q. L. Li, and W. Q. Fan, *J. Heterocycl. Chem.*, **25**, 1287 (1988).
20 M. Irie and M. Kato, *J. Am. Chem. Soc.*, **107**, 1024 (1985).
21 T. Yamaguchi, T. Seki, T. Tamaki, and K. Ichimura, *Bull. Chem. Soc. Jpn.*, **65**, 649 (1992).
22 T. Seki, T. Tamaki, T. Yamaguchi, and K. Ichimura, *Bull. Chem. Soc. Jpn.*, **65**, 657 (1992).
23 L. Fitjer, R. Gerke, W. Lüttke, P. Müller, and I. Usón, *Tetrahedron*, **55**, 14421 (1999).
24 K. Eggers, T. M. Fyles, and P. J. Montoya-Pelaez, *J. Org. Chem.*, **66**, 2966 (2001).
25 M. Kasha, *J. Chem. Soc., Faraday Trans. 2*, **82**, 2379 (1986).
26 Y. Norikane, H. Itoh, and T. Arai, *J. Phys. Chem. A*, **106**, 2766 (2002).
27 T. Suzuki, Y. Kaneko, and T. Arai, *Chem. Lett.*, **2000**, 756.
28 M. Ikegami and T. Arai, *Chem. Lett.*, **2000**, 996.
29 M. Ikegami and T. Arai, *J. Chem. Soc., Perkin Trans. 2*, **2002**, 1296.
30 J. Bergman, *Tetrahedron Lett.*, **46**, 4723 (1972).
31 D. F. Eaton, *Pure Appl. Chem.*, **60**, 1107 (1988).
32 S. L. Murov, I. Carmichael, and G. L. Hug, "Handbook of Photochemistry," 2nd ed, Marcel Dekker, New York (1993).
33 H. E. Kissinger, *Anal. Chem.*, **29**, 1702 (1957).
34 T. Yatsuhashi and H. Inoue, *J. Phys. Chem. A*, **101**, 8166 (1997).
35 T. Yatsuhashi, Y. Nakajima, T. Shimada, and H. Inoue, *J. Phys. Chem. A*, **102**, 3018 (1998).
36 E. C. Lim, *J. Phys. Chem.*, **90**, 6770 (1986).
37 T. Yoshihara, H. Shimada, H. Shizuka, and S. Tobita, *Phys. Chem. Chem. Phys.*, **3**, 4972 (2001).
38 F. D. Lewis, R. S. Kalgutkar, and J. S. Yang, *J. Am. Chem. Soc.*, **123**, 3878 (2001).